Received 25 August 2023; revised 9 October 2023; accepted 24 October 2023. Date of publication 28 November 2023; date of current version 30 January 2024.

Digital Object Identifier 10.1109/OJAP.2023.3332846

Design of a Dual-Branch Resonator End-Launcher for Low-Loss WBAN Communications Using Wearable Waveguide Surfaces

MARIA EL BACHA (Student Member, IEEE), FABIEN FERRERO (Member, IEEE), AND LEONARDO LIZZI (Senior Member, IEEE)

Université Côte d'Azur, CNRS, LEAT, 06903 Sophia Antipolis, France

CORRESPONDING AUTHOR: F. FERRERO (e-mail: fabien.ferrero@univ-cotedazur.fr)

This work was supported in part by the French Agence nationale de la recherche and Direction générale de l'Armement (DGA) under Grant ANR-17-CE24-0013, and in part by the Le Centre de REcherche Mutualisé sur les ANTennes (CREMANT).

ABSTRACT Wearable waveguide surfaces can be integrated into textiles to improve Wireless Body Area Networks (WBANs). In this work, a compact 30 mm x 30 mm dual-branch resonator end-launcher to enable communication through a waveguide surface manufactured with textile-compatible material at 2.4GHz is proposed. A 25 mm x 25 mm clearance zone area is respected for electronic component integration. The end-launcher topology uses a balanced dual-branch configuration to maximize electromagnetic coupling with the flexible waveguide surface. A design methodology is proposed to co-design the end-launcher and the waveguide surface. Experimental measurements on the human body torso are presented with 0.3 dB/cm insertion loss between 2.4 and 2.48 GHz. The final result is an autonomous, compact, wireless-contact, and battery-powered end-launcher for innovative clothing applications.

INDEX TERMS Antennas, coupling, dual-branch resonator, end-launcher, human body torso, on-body communication, waveguide surface, wearable.

I. INTRODUCTION

WEARABLE technology has witnessed historical growth, with a total market worth nearly $80bn in 2020 and expected to reach $138bn by 2025. The market mainly drives this phenomenon with smartwatches, hearables, skin patches, other medical patient monitoring devices, virtual reality headsets, smart clothing, over-the-counter hearing aids, or smart contact lenses [1]. In wireless body area networks (WBANs), sensors are considered the key for any application purpose. Most of the products listed above rely on central sensors that can communicate with the user's body and environment to function properly [2].

The greatest challenge for wearable technologies is their proximity to the human body. Such proximity can harm human health and the antenna's performance by affecting electromagnetic (EM) wave propagation. Wearable waveguide surfaces represent a very interesting solution to solve this issue. Waveguiding surfaces usually include a ground plane that provides shielding, prevents electromagnetic radiation from penetrating the human tissue, and protects the communication from the lossy dielectric properties of the human body [3]. In addition, the ground plane can enhance communication as it can be exploited to confine and guide EM waves between wearable devices, thus improving the communication rate and the whole system's efficiency [4].

Different antenna designs and topologies have been fabricated and studied in order to assure an effective coupling with the waveguide surfaces, thus acting as end-launchers for EM wave propagation. Whatever the application, dipoles and monopoles are considered the most common antenna types used to excite a waveguide surface (as in [5], [6], [7], [8], [9]). For example, a coplanar waveguide monopole antenna was designed in [7] to enhance the transmission rate over an artificial magnetic conductor (AMC) waveguide jacket. A textile diamond dipole antenna was conceived to improve the transmission between antennas over a waveguide surface [8]. Another dipole antenna was used in [9] over a meander spoof surface plasmon polariton (SSPP) to excite

the propagating mode. Small (1-inch long) antennas were implemented in [10] for transmission measurements over a metamaterial textile surface plasmon structure for on-body wireless communication at 2.4 GHz.

This paper aims to present the design of an end-launcher that can reach higher coupling with a waveguide surface and, therefore, enable a higher transmission rate for the desired on-body communication.

We have previously developed a 66×8 mm^2 planar printed dipole [11] that couples with the waveguide surface designed in [12]. With this end-launcher, the measured transmission rate reached -8 dB over 43 cm distance. However, dipoles depend on their feeding on a cable and do not have enough space to integrate electronics. This means that the overall system is not suitable for wireless and autonomous applications, as needed, for example, by smart clothes applications. We have also developed another 30×30 mm^2 compact IFA antenna in [13] that also couples with the same waveguide surface for on-body communication. The advantage of this design is its adequate space for the electronics. However, the coupling could be highly improved, as the transmission rate suffers from significant variations (around 7 dB) over the 2.4-2.47 GHz frequency band. Accordingly, a new end-launcher is designed and proposed in this paper.

The new end-launcher is a dual-branch resonator inspired by the dipole's characteristics and functioning mechanism that will communicate through the waveguide surface designed in [12]. The waveguide surface is modeled by 3 rows of 33 periodic patches positioned on a 3.2 mm thick polar tissue substrate ($\varepsilon_r = 1.1$) backed by a ground plane layer. The end-launcher is electromagnetically coupled to the waveguide surface, to generate a guided EM wave traveling towards a second end-launcher (acting as a receiver), and assures the wave propagation from one end to another. A 25×25 mm^2 terminal form factor is targeted to support a miniature battery and electronic components for Bluetooth integration. The result is an autonomous, compact, miniaturized, wireless-contact, and battery-powered end-launcher for smart clothing applications.

This paper is organized as follows. Section II is dedicated to the dual-branch resonator's methodology and design through two major phases: in free space and over the waveguide surface. The effectiveness of the design is experimentally validated in both planar and curved scenarios, as detailed in Section III, with the integration of a full textile waveguide surface. Finally, some conclusions are drawn in Section IV.

II. DUAL-BRANCH RESONATOR END-LAUNCHER DESIGN

This section is dedicated to the design of the end-launcher. More specifically, it presents the end-launcher concept, the design methodology, and its simulated performance in both free space and over the waveguide surface.

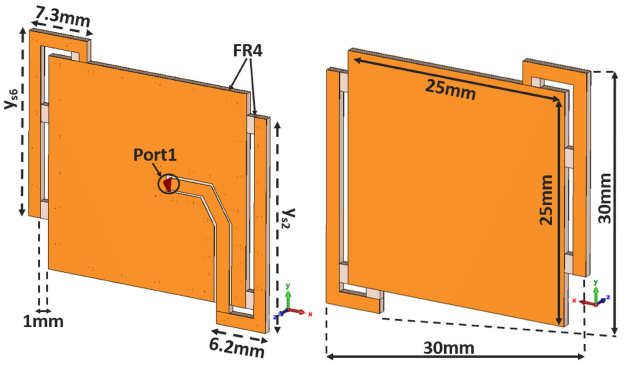

(a) Front View (b) Back View

FIGURE 1. Dual-branch resonator end-launcher structure.

A. END-LAUNCHER CONCEPT

This section presents the end-launcher concept covering the ISM band (2.4-2.48 GHz). A 25×25 mm^2 space is reserved for RF and electronic components. The radiating elements of this structure are the dual branches that are located at the two diagonally opposite corners of the structure. A 0.8mm thick FR4 substrate separates the top from the bottom of the end-launcher. A grounded coplanar waveguide is used to feed the antenna. Due to the sensibility of this structure, the substrate was partially removed between the radiating elements and the patch terminal. Considering its fragility, some substrate scraps were left to keep the structure rigid. The end-launcher structure is shown in Fig. 1.

A dual-branch approach is adopted in this model. This model is the result of a study considering several end-launcher structures, in which the objective was to maximize the coupling with the waveguide surface while keeping enough space for electronics integration. According to the design presented in [13], one branch is insufficient to attain the highest transmission rate. it makes it challenging to obtain a stable transmission behavior over 50 MHz of frequency range. In addition, a high transmission level is attained with dipoles as end-launchers [11]. So this design combines both models: a double branch dipole-inspired radiating solution and a terminal where the electronics can be integrated.

B. DESIGN METHODOLOGY

The design of the end-launcher is done through a 2-steps methodology, starting from a design in free space and then the study and the tuning on the waveguide surface.

In free space, the reflection coefficient $|S_{11}|$ of the end-launcher must be matched with the -6 dB criteria in the ISM band (2.4-2.48 GHz). The optimization of the end-launcher is done through different parametric studies. This part will be developed in the following section. The end-launcher must also meet some major requirements: it must be (a) miniaturized but also have enough space for electronic components, (b) autonomous, allowing for battery integration, and (c) wireless, so without the need for a

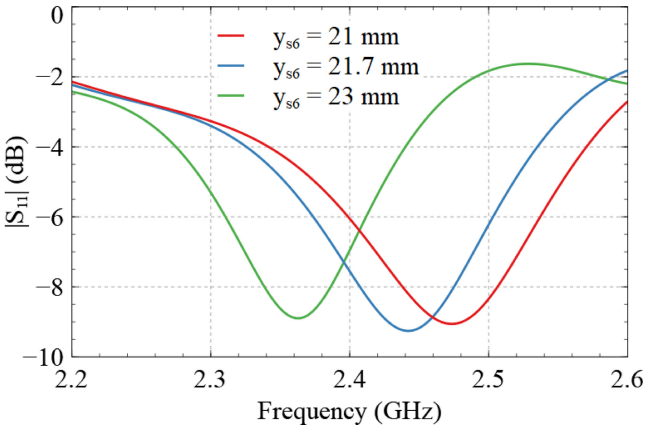

FIGURE 2. End-launcher impedance matching for different y_{s6} values.

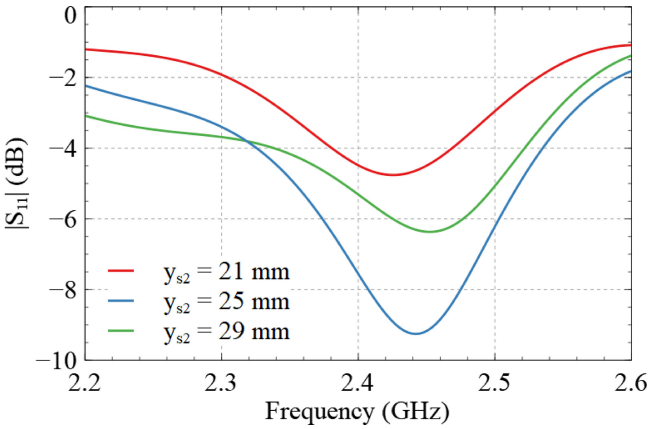

FIGURE 3. End-launcher impedance matching for different y_{s2} values.

feeding cable. It should also have a dipole-like double-branch design for better coupling with the waveguide surface thus, enabling a high transmission rate (high $|S_{21}|$).

The next step is the optimization of the end-launcher on the waveguide surface. Towards this end, two major studies have to be performed. One deals with the position of the end-launcher on the waveguide surface, especially in terms of x and y directions. The best position will determine the highest coupling and, thus, the highest transmission rate. The E-field propagation should be from one end to the other end all along the waveguide surface. The other one concerns the fine-tuning of the end-launcher geometrical parameters to maximize the average $|S_{21}|$ value in the ISM frequency band.

C. FREE SPACE DESIGN

The radiating and electric characteristics of the end-launcher have been initially optimized in free space mainly through the variation of two important parameters: y_{s6} (Fig. 2) and y_{s2} (Fig. 3).

1) PARAMETER Y_{S6}

This parameter indicates the length of the branch that is not fed. It is in charge of shifting the frequency to the desired working band. Different values were tested (Fig. 2). With $y_{s6} = 21.7$ mm, the resonant frequency is at 2.45 GHz covering the 2.38 - 2.5 GHz band ($|S_{11}| \leq -6$ dB). For $y_{s6} = 21$ mm and $y_{s6} = 23$ mm, the reflection coefficient $|S_{11}|$ is centered at 2.48 GHz and 2.38 GHz, respectively.

2) PARAMETER Y_{S2}

The length of the feeding branch is defined by the y_{s2} parameter. The value of y_{s2} controls the matching of the antenna. The red and blue curves in Fig. 3 represent the reflection coefficient $|S_{11}|$ for $y_{s2} = 21$ mm and $y_{s2} = 29$ mm, respectively. As can be seen, the antenna is not adapted to 50Ω for those values. For $y_{s2} = 25$ mm, the $|S_{11}|$ blue curve falls below -6 dB.

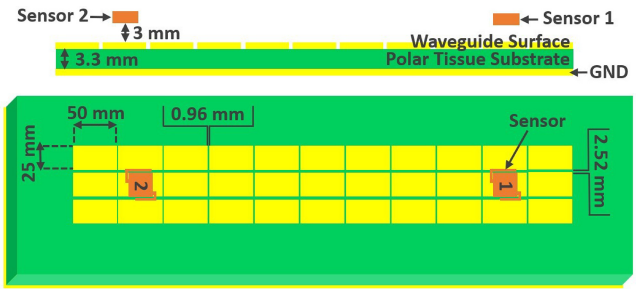

FIGURE 4. Waveguide surface structure.

D. OVER THE WAVEGUIDE SURFACE

The dual-branch resonator was designed and studied in free space in the previous section. However, this work aims to enable the on-body communication between two end-launchers through a waveguide surface. So, two copies of the dual-branch resonator have been positioned above the two ends of the waveguide surface designed in [12]. More details about the design of the waveguide surface structure can be found in [12]. Their communication is evaluated through the transmission coefficient between the two end-launchers. The waveguide surface (Fig. 4) comprises three layers: a ground plane, a 3.3 mm Polar Tissue substrate, and three rows of periodic patches that constitute the guiding structure with 55.9 cm of distance between the first and the last patch. The patch size is 50×25 mm^2.

1) POSITION STUDY

Placing the end launchers on the waveguide surface is neither easy nor by default. It needs a whole study in x, y, and z directions to ensure that they are in the position that couples the best with the waveguide surface to ensure the highest transmission rate. The position sensitivity study reported here only concerns the y-direction with four different positions with a step of 25 mm, as shown in Fig. 5. On the x-axis, the end-launcher is centered on the second row of the waveguide surface to maintain symmetry. As shown in [11], where a full study of the end-launcher position in the x, y, and z-axis was presented, the displacement sensitivity in the z-axis is very low and does not affect the system's performance.

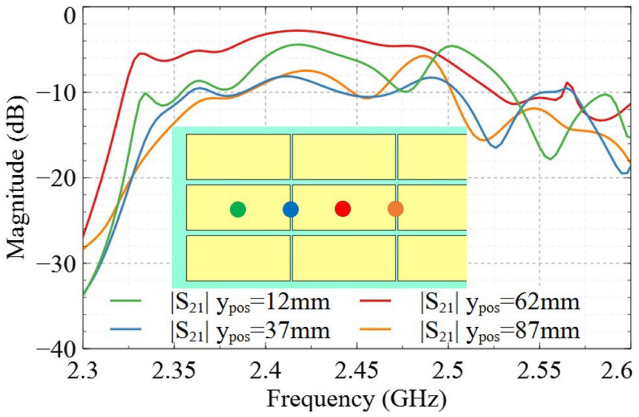

FIGURE 5. Transmission coefficient behavior for different positions of the end-launcher on the waveguide surface.

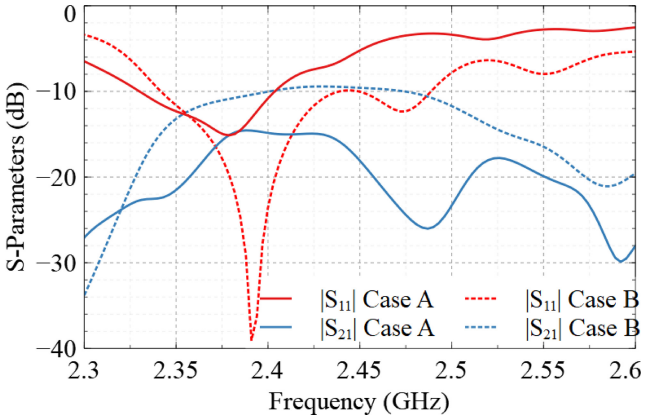

FIGURE 6. Impedance matching and transmission coefficient behaviors for Case A and B.

In Fig. 5, the circles represent the center of the sensor's position. The colors are differentiated according to the parameter's $|S_{21}|$ curve legend. The first position is $y_{pos} = 12$ mm, which represents the end-launcher placed in the center of the first patch. A maximum of -4.5 dB in terms of transmission coefficient is obtained at 2.4 and 2.5 GHz, with a minimum of -10 dB at 2.48 GHz. The operating frequency band (transmission coefficient > -10 dB) is from 2.35 to 2.57 GHz. When the sensor's center is placed between the first and the second patches ($y_{pos} = 37$ mm), the maximum transmission value is -8 dB over 2.36 - 2.51 GHz.

The third position of the sensor is the center of the second patch, represented by the red curve ($y_{pos} = 62$ mm). In this case, the transmission coefficient reaches -3 dB at 2.42 GHz with a frequency band of 2.32 - 2.52 GHz. The last position is $y_{pos} = 87$ mm with the orange circle representing the center of the sensor placed above the gap between the second and the third patch. A transmission coefficient peak is at -6 dB at 2.48 GHz with a band of 2.39 - 2.5 GHz. In this case, the transmission coefficient reaches provides the best coupling between the end-launcher and the waveguide surface, thus resulting in the highest transmission coefficient and communication rate.

2) GEOMETRICAL PARAMETERS STUDY

Once the optimal end-launcher position has been identified, a retuning of the geometrical model is necessary in order to get the highest coupling with the waveguide surface and the highest transmission rate.

Case A in Fig. 6 represents the dual-branch resonator optimized in free space (with $y_{s6} = 21.7$ mm and $y_{s2} = 25$ mm) placed on the waveguide surface at its optimal position. Case B deals with the re-tuned dual-branch resonator (with $y_{s6} = 20$ mm and $y_{s2} = 24$ mm) placed at the same optimal position (center of the second patch).

As it can be observed, the re-optimization of the end-launcher structure, taking into account the presence of the waveguide surface (case B), allows an increase of 5 dB in the transmission coefficient (considering that the $|S_{21}|$ level attained by the case A configuration is never better than -15 dB). This difference can be ascribed to the variation of the reflection coefficient: the $|S_{11}|$ for case B is matched at -15 dB, covering 2.34 - 2.4 GHz, while the reflection coefficient for case A is much higher over the same band.

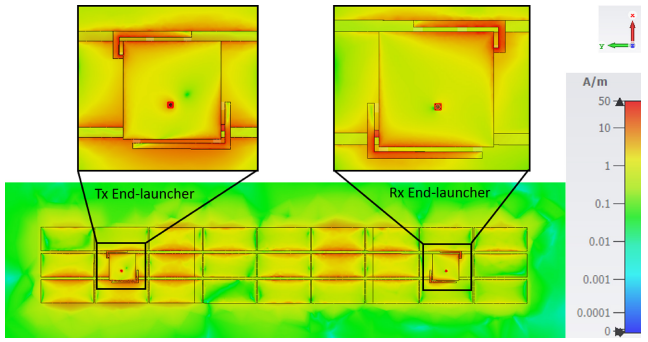

FIGURE 7. Surface current distribution on the end-launcher and the guiding structure at 2.45 GHz.

To clearly understand the propagation mechanism, Fig. 7 shows the surface current distribution at 2.45 GHz. Both branches of the transmitting end-launcher are excited. This allows the end-launcher to couple to the waveguide surface where the guided wave propagates all along the surface to reach the receiving end-launcher, where both branches are excited as well.

3) RADIATION BEHAVIOR

The radiation pattern of the end-launcher over body with and without the waveguided surface is shown in Fig. 8. As expected, the radiation with the waveguided structure is higher than the one without the structure as part of the energy is absorbed by the human body.

III. EXPERIMENTAL VALIDATION

After having numerically evaluated the structure's performance, experimental investigations are conducted through prototyping and measurements in the sections below.

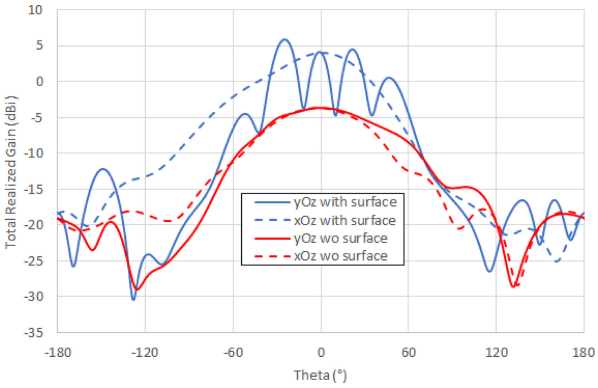

FIGURE 8. Simulated end-launcher radiation pattern with and without the waveguided surface over the human body.

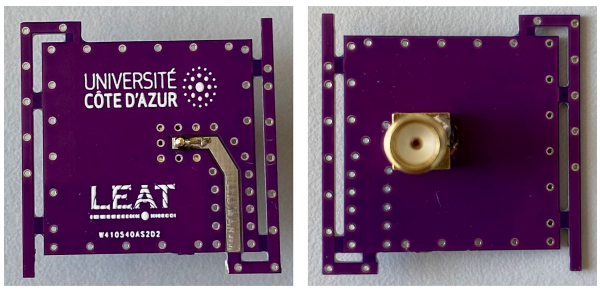

(a) Front View (b) Back View

FIGURE 9. End-launcher prototype.

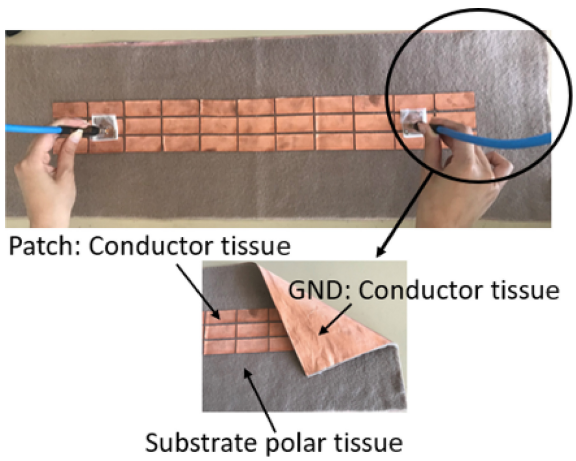

FIGURE 10. Textile waveguide surface prototype.

A. PLANAR SCENARIO

Prototypes of the waveguide structure and the end-launcher have been realized. The prototype of the dual-branch resonator is shown in Fig. 9. As presented in Fig. 10, the waveguide surface prototype is 100% textile. A conductor textile tissue is used for the metallic parts (the patches and the ground plane), while the substrate is made from polar tissue with a thickness of 3 mm. The planar scenario of Fig. 10 was tested and measured using a VNA. A transmission coefficient higher than −10 dB is obtained in the large band from 2.5 GHz to 2.65 GHz (Fig. 11).

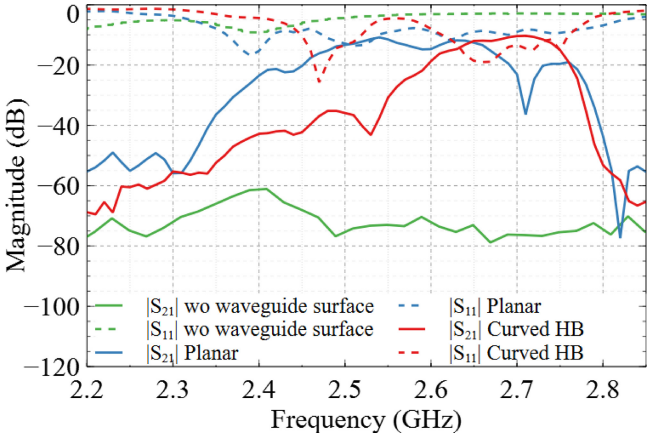

FIGURE 11. S-Parameters measurements.

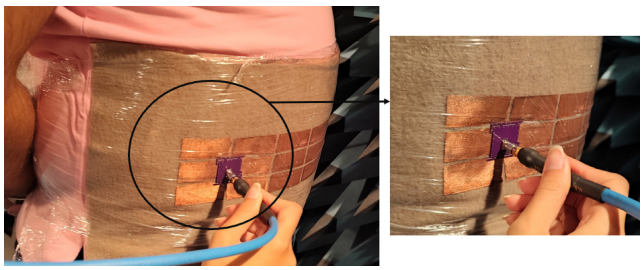

FIGURE 12. Measurements on the human body torso.

B. CURVED ON-BODY SCENARIO

The structure shown in Fig. 10 was fixed with cellophane paper around the human body torso (Fig. 12) to perform the on-body measurements. It is important to well-fix and to stabilize the structure to control the elasticity of the polar tissue. Otherwise, risks of breaking the periodicity of the structure can occur. This would reduce the EM wave guidance of the waveguide surface, thus generating a lower communication rate.

A transmission coefficient reaching −10 dB is observed as in the case of the planar measurements. However, this value is obtained with an 80 MHz frequency shift (from 2.63 GHz to 2.71 GHz) and lower operating bandwidth: 190 MHz for the planar scenario (from 2.47 to 2.66 GHz) and 140 MHz (from 2.61 to 2.75 GHz) for the curved one (Fig. 11). The reason behind the frequency shifting is the gap that extends with the curved scenario because of the elasticity of the substrate that causes the stretching.

Finally, for the sake of comparison, the transmission coefficient has been measured also when the waveguide surface is not present (green curve in Fig. 11). An average of −70 dB of transmission coefficient is obtained with a maximum at 2.4 GHz (the resonant frequency of the end-launcher). This highlights the role and importance of employing a waveguide surface to improve the quality of wireless on-body communications.

IV. CONCLUSION

A 30 x 30 mm^2 Dual-branch resonator end-launcher is designed for wireless on-body communication (side

TABLE 1. Performance comparison with state of the art.

Parameters	[7]	[10]	[12]	This work
End-launch Max Dimensions*	0.431λ	0.203λ	0.563λ	0.244λ
Center Frequency (MHz)	2450	2400	2500	2680
-3dB Freq. Bandwidth (MHz)	180	189	120	130
Port to Port distance (mm)	104	100	435	304
Bending Radius (mm)	/	/	150	150
Normalized $\lvert S_{21}\rvert$ (dB/cm)	-0.6	-3	-0.18	-0.25
Textile	YES	YES	NO	YES

* λ *is the wavelength at the center frequency.*

dimension of 0.244λ). The design of this antenna is done firstly in free space and then over the waveguide surface. The dual-branch resonator is miniaturized, designed to have enough space (25 x 25 mm^2) for integrating electronic components such as battery and BLE microcontroller for the seek of autonomous and wireless characteristics. The high coupling with a waveguide surface at 2.4 - 2.48 GHz frequency band provides a high transmission coefficient (around -10 dB) and, thus, a low loss communication rate (0.3 dB/cm). The effectiveness of the suggested structure is demonstrated by the comparison with various systems that aim for on-body communications (Table 1).

An innovative 100% textile fabric material prototype was fabricated and measured in planar and on-body curved scenarios to validate numerical results and prove the relevance of implementing a waveguide surface (50 dB gain in terms of insertion loss). Despite the difficulty of fabrication, this prototype directly targets e-clothes due to its flexibility and integration capacity.

REFERENCES

[1] IDTechEx Ltd. "Wearable sensors 2021-2031." IDTechEx.com. Accessed: Jul. 26, 2022. [Online]. Available: https://www.idtechex.com/en/research-report/wearable-sensors-2021-2031/780

[2] IDTechEx Ltd. "Wearable technology forecasts 2021-2031." IDTechEx.com. Accessed: Jul. 26, 2022. [Online]. Available: https://www.idtechex.com/en/research-report/wearable-technology-forecasts-2021-2031/839

[3] D. Sievenpiper, L. Zhang, R. F. J. Broas, N. G. Alexopolous, and E. Yablonovitch, "High-impedance electromagnetic surfaces with a forbidden frequency band," *IEEE Trans. Microwave Theory Tech.*, vol. 47, no. 11, pp. 2059–2074, Nov. 1999.

[4] M. S. Alam, N. Misran, B. Yatim, and M. T. Islam, "Development of electromagnetic band gap structures in the perspective of microstrip antenna design," *Int. J. Antennas Propag.*, vol. 2013, pp. 1–23, Apr. 2013.

[5] K. Zhang, G. A. E. Vandenbosch, and S. Yan, "A novel design approach for compact wearable antennas based on metasurfaces," *IEEE Trans. Biomed. Circuits Syst.*, vol. 14, no. 4, pp. 918–927, Aug. 2020.

[6] K. Kamardin, M. K. A. Rahim, N. A. Samsuri, M. E. Jalil, and H. A. Majid, "Transmission enhancement using textile artificial magnetic conductor with coplanar waveguide monopole antenna," *Microw. Opt. Technol. Lett.*, vol. 57, pp. 197–200, Jan. 2015.

[7] O. A. Saraereh, I. Khan, B. M. Lee, and A.K.S. Al-Bayati, "Modeling and analysis of wearable antennas," *Electronics*, vol. 8, no. 1, pp. 1–12, 2019.

[8] M. A. Abdullah, M. K. A.Rahim, and N. A. Samsuri, "Positions of dual-band textile diamond dipole antenna with dual-band textile artificial magnetic conductor waveguide sheet for body centric communication," *Elektrika*, vol. 16, no. 1, pp. 35–38, Apr. 2017.

[9] A. Ghaddar, É. Lheurette, and L. Burgnies, "Wireless experimental determination of dispersion curves of spoof surface plasmon polariton modes supported by a transmission line," *Phys. Status Solidi B*, vol. 258, no. 6, 2021, Art. no. 2100003.

[10] X. Tian et al., "Wireless body sensor networks based on metamaterial textiles," *Nature Electron.*, vol. 2, no. 6, pp. 243–251, 2019.

[11] M. El Bacha, F. Ferrero, and L. Lizzi, "Influence of end-launch position over a Textile Wave-guide surface for BAN applications," in *Proc. 15th Eur. Conf. Antennas Propag. (EuCAP)*, 2021, pp. 1–4.

[12] M. El-Bacha, F. Ferrero, and L. Lizzi, "Wearable waveguide surface for low-loss body area network communications," *IEEE Antennas Wireless Propag. Lett.*, vol. 20, no. 12, pp. 2295–2299, Dec. 2021.

[13] M. El Bacha, F. Ferrero, and L. Lizzi, "Compact waveguide surface end-launcher suitable for wearable body area network terminals," in *Proc. IEEE Int. Symp. Antennas Propag. USNC-URSI Radio Sci. Meet. (APS/URSI)*, 2021, pp. 413–414.

MARIA EL BACHA (Student Member, IEEE) received the master's degree in telecommunication and networking engineering from Antonine University, Lebanon, in 2019, and the Ph.D. degree in electronics from the Laboratory of Electronics, Antennas, and Telecommunications, Unicersité Côte d'Azur, France, in 2022. Her research focuses on wearable end-launchers coupled with waveguide surfaces for WBAN communications.

FABIEN FERRERO (Member, IEEE) received the Ph.D. degree in electrical engineering from the University of Nice-Sophia Antipolis in 2007. From 2008 to 2009, he worked with IMRA Europe (Aisin Seiki Research Center) as a Research Engineer and developed automotive antennas. In 2010, he is recruited as an Associate Professor with the Polytechnic School, Université Nice Sophia-Antipolis. Since 2018, he has been a Full Professor with Université Côte d'Azur. He is doing his research with Laboratoire d'Electronique, Antennes et Telecommunications. His studies concerned the design and measurement of millimetric antennas, IoT systems, and space applications.

LEONARDO LIZZI (Senior Member, IEEE) received the master's degree in telecommunication engineering and the Ph.D. degree in information and communication technology from the University of Trento, Italy, in 2007 and 2011, respectively. He is currently an Associate Professor with University Côte d'Azur (UCA), France. During his Ph.D., he has been a Visiting Researcher with Pennsylvania State University, USA, and the University of Nagasaki, Japan. From 2011 to 2014, he was a Postdoctoral Researcher with the Laboratory of Electronics, Antennas, and Telecommunications, UCA. He is the coordinator of the European School of Antennas Ph.D. course on "Antennas and Rectennas for IoT Applications." He is the coauthor of more than 140 papers in international journals and conference proceedings. At the moment, his research focuses on reconfigurable, miniature, multistandards antennas for Internet of Things applications, wearable devices, and 5G terminals.